Approximated fast estimator for the shape parameter of generalized Gaussian distribution for a small sample size

R. KRUPIŃSKI*

West-Pomeranian University of Technology in Szczecin, Chair of Signal Processing and Multimedia Engineering,
10 26-Kwietnia St., 71-126 Szczecin, Poland

Abstract. Most estimators of the shape parameter of generalized Gaussian distribution (GGD) assume asymptotic case when there is available infinite number of observations, but in the real case, there is only available a set of limited size. The most popular estimator for the shape parameter, i.e., the maximum likelihood (ML) method, has a larger variance with a decreasing sample size. A very high value of variance for a very small sample size makes this estimation method very inaccurate. A new fast approximated method based on the standardized moment to overcome this limitation is introduced in the article. The relative mean square error (RMSE) was plotted for the range 0.3–3 of the shape parameter for comparison with other methods. The method does not require any root finding, any long look-up table or multi step approach, therefore it is suitable for real-time data processing.

Key words: estimation, generalized Gaussian distribution, standardized moment, approximated fast estimator.

1. Introduction

Most of the estimation methods for the shape parameter of GGD assume that the sample size is large. The estimation of GGD parameters may be carried out by the use of ML method [1], the moment method (MM) [2], entropy matching [3]. For all these methods the existence and the uniqueness of the parameters are based on asymptotic behavior, i.e., the sample size is sufficiently large. In [4], it was shown that the computation of GGD parameters on small samples is not the same as on larger ones. The authors presented a necessary and sufficient condition for the existence of the parameters in a maximum likelihood framework. GGD was observed to appear in many signal and image processing applications. A large sample size very often is not available. Therefore, the relaying method for the estimation of GGD shape parameter is necessary.

The ML method used for the estimation of the shape parameter is complex and time consuming. The complexity can be reduced by the application of the One Moment (OM) method [5]. Instead of the ML method the Mallat's method is often used for estimation, even though the method is not accurate for the whole range of the shape parameter [6].

In [7], the scale-invariant fourth moment is used as an accurate initial value to the Newton–Raphson iteration in the estimation parameters of complex GGD.

The method [6] based on the approximation of the moment method in four intervals allows fast estimation of GGD shape parameter for real-time applications and requires storing only twelve coefficients. The authors presented the method which approximates the estimation of GGD shape parameter in the range 0.3–3.

A review of the different approaches to shape parameter estimation problems can be found in [8]. The authors stated that the estimators (the Mallat's generalized Gaussian ratio method (MRM), the kurtosis generalized Gaussian ratio method (KRM)) were still not satisfactory in the case of short data. The negentropy matching (NM) method can still accurately estimate the parameters for small sample size, but for the shape parameter $p < 1$.

The peaky distributed signals can be observed in many signal processing applications [9, 10].

In Sec. 2 the estimation methods of GGD shape parameter and an approximation model for a small sample size are discussed. In Sec. 3 the numerical results are presented.

The methods based on the root finding may not have a real root for a small sample size created from simulated observations. In Sec. 3 it can be observed that this situation appeared for the ML method for $N < 60 \land p = 0.4$, $N < 85 \land p = 1$ and $N < 120 \land p = 2$.

2. Material and methods

The probability density function (PDF) of the continuous random variable of GGD [11] takes the form

$$f(x) = \frac{\lambda(p,\sigma) \cdot p}{2 \cdot \Gamma\left(\frac{1}{p}\right)} e^{-[\lambda(p,\sigma) \cdot |x-\mu|]^p}, \tag{1}$$

where $\Gamma(z) = \int_0^\infty t^{z-1} e^{-t} dt$, $z > 0$, is the Gamma function [12], p denotes the shape parameter, μ is the location

*e-mail: rkrupinski@wp.pl

parameter and λ relates to the variance of the distribution and can be calculated from

$$\lambda(p,\sigma) = \frac{1}{\sigma}\left[\frac{\Gamma\left(\frac{3}{p}\right)}{\Gamma\left(\frac{1}{p}\right)}\right]^{1/2}, \tag{2}$$

where σ denotes the standard deviation. The special case of GGD can be observed when the shape parameter equals $p = 1$ and $p = 2$, which corresponds to Laplacian and Gaussian distributions respectively. For $p \to 0$, $f(x)$ approaches an impulse function, and for $p \to \infty$, $f(x)$ approaches a uniform distribution. For $\mu = 0$, the probability density function is centered around zero.

From the definition of absolute moment

$$E\left[|X|^m\right] = \int_{-\infty}^{\infty} |x|^m \cdot f(x)dx,$$

for GGD the following is obtained [13]

$$E_m = \frac{\Gamma\left(\frac{m+1}{p}\right)}{\lambda^m \cdot \Gamma\left(\frac{1}{p}\right)}, \tag{3}$$

where m can be a real number.

The E_m estimated value of the moment can be acquired from the equation

$$\widehat{E}_m = \frac{1}{N} \cdot \sum_{i=1}^{N} |x_i|^m \tag{4}$$

and where N denotes the number of observed variables, and $\{x_1, x_2, \ldots, x_N\}$ is the collection of N i.i.d zero-mean random variables.

The presented model [6] for the approximated estimation of GGD shape parameter is derived from two moments method and is calculated for the selected intervals related to the shape parameter

$$\widehat{p} = \left(\frac{\log(Gp) - a}{b}\right)^{1/c}, \tag{5}$$

where

$$Gp = \frac{E_{m_1}}{(E_{m_2})^{\frac{m_1}{m_2}}} \tag{6}$$

and $\widehat{p}$ denotes the estimated value of the shape parameter, E_{m_1} and E_{m_2} are the estimated values of the moments, which can be found from Eq. (4). The parameters a, b and c are set independently for each interval and both their values and the procedure for their selection are discussed in [6].

Du [1] described the estimation of the shape parameter derived from the maximum likelihood method

$$\frac{\Psi\left(1 + \frac{1}{p}\right) + \log(p)}{p^2} + \frac{1}{p^2}\log\left(\frac{1}{N}\sum_{i=1}^{N}|x_i|^p\right)$$

$$-\frac{\sum_{i=1}^{N}|x_i|^p \log(|x_i|)}{p\sum_{i=1}^{N}|x_i|^p} = 0, \tag{7}$$

where

$$\Psi(\tau) = -\gamma + \int_0^1 (1 - t^{\tau-1})(1 - t)^{-1}dt \tag{8}$$

and $\gamma = 0.577\ldots$ denotes the Euler constant. The root of Eq. (7) gives the ML estimate $\widehat{p}$.

Equation (3) for two different moment values m_1 and m_2 and eliminating λ leads to:

$$g = \frac{\Gamma\left(\frac{m_2+1}{p}\right)\Gamma\left(\frac{1}{p}\right)^{\frac{m_2}{m_1}-1}}{\Gamma\left(\frac{m_1+1}{p}\right)^{\frac{m_2}{m_1}}} = \frac{E_{m_2}}{(E_{m_1})^{\frac{m_2}{m_1}}}, \tag{9}$$

which is the method for the estimation of the shape parameter based on two moments. The inverse function to the g function, Eq. (9), depends on the moment values m_2 and m_1 and can be approximated as follows:

- $m_1 = 0.25$ and $m_2 = 0.5$

$$\widehat{p}_0 = \begin{cases} 55 \cdot g^{-70} + 0.73, & \text{for } g < 1.079 \\ 5.7 \cdot g^{-28} + 0.315, & \text{for } g \geq 1.079 \\ & \wedge g < 1.132 \\ 2.05 \cdot g^{-15} + 0.18, & \text{for } g \geq 1.132 \end{cases}, \tag{10}$$

- $m_1 = 0.5$ and $m_2 = 1$

$$\widehat{p}_1 = \begin{cases} 26 \cdot g^{-18} + 0.67, & \text{for } g < 1.27 \\ 5.5 \cdot g^{-9} + 0.365, & \text{for } g \geq 1.27 \end{cases}, \tag{11}$$

- $m_1 = 1$ and $m_2 = 2$

$$\widehat{p}_2 = \begin{cases} 29 \cdot g^{-7} + 0.8, & \text{for } g < 2 \\ 5 \cdot g^{-3} + 0.37, & \text{for } g \geq 2 \end{cases}, \tag{12}$$

- $m_1 = 2$ and $m_2 = 3$

$$\widehat{p}_3 = \begin{cases} 77 \cdot g^{-10} + 1.275, & \text{for } g < 1.6 \\ 16.3 \cdot g^{-5.5} + 0.748, & \text{for } g \geq 1.6 \end{cases}, \tag{13}$$

- $m_1 = 2$ and $m_2 = 4$

$$\widehat{p}_4 = \begin{cases} 12 \cdot g^{-1.98} + 0.64, & \text{for } g < 6 \\ 6 \cdot g^{-1.3} + 0.42, & \text{for } g \geq 6 \end{cases}, \tag{14}$$

-

$$\widehat{p}_{04} = 0.5 \cdot (\widehat{p}_0 + \widehat{p}_4). \tag{15}$$

Equation (14) for two moments $m_1 = 2$ and $m_2 = 4$ corresponds to kurtosis. The inverse function of Eq. (9) for two moments $m_1 = 2$ and $m_2 = 4$ is depicted in Fig. 1.
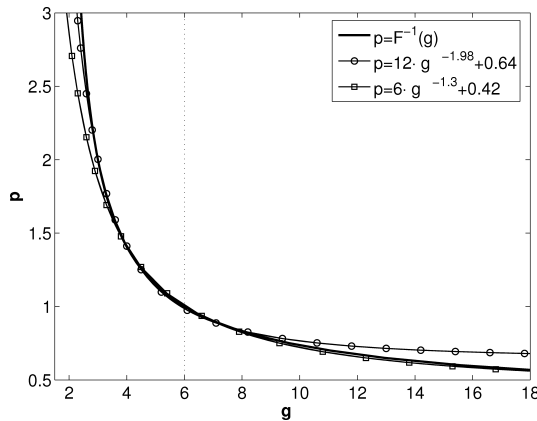

Fig. 1. Inversion function of Eq. (9) for two moments $m_1 = 2$ and $m_2 = 4$ and two components from Eq. (14)

Additionally, in the same figure two components approximating this function from Eq. (14) are overlaid with a threshold value $g = 6$. It can be noticed that the inverse function is better approximated by one component over the threshold value $g = 6$ and by another component below this value. It should be pointed out that the model used for the approximation of inverse function to the g function (Eq. (9)) in this article is different than the model introduced in [6] (Eq. (5)). Equations (10)–(15) were obtained by fitting the inverse function of Eq. (9) to the model $a \cdot g^{-b} + c$.

Authors also examined other sets for the moment orders: $m_1 = 0.1$ and $m_2 = 0.5$; $m_1 = 0.125$ and $m_2 = 0.25$. Nevertheless, Eqs. (10)–(15) became the most usable in the final estimation, i.e, led to the smallest error. The final estimation $\widehat{p}_S$ can be found from the following relation:

$$\widehat{p}_S = \begin{cases} \widehat{p}_4, & \text{for } \widehat{p}_1 \geq 1.86 \\ \widehat{p}_{04}, & \text{for } 1.04 \leq \widehat{p}_1 < 1.86 \\ \widehat{p}_1, & \text{for } 0.57 \leq \widehat{p}_1 < 1.04 \\ \widehat{p}_0, & \text{for } \widehat{p}_1 < 0.57 \end{cases}, \quad (16)$$

where $\widehat{p}_0$, $\widehat{p}_1$, $\widehat{p}_{04}$ and $\widehat{p}_4$ are defined by Eqs. (10), (11), (15) and (14) respectively. $\widehat{p}_1$ has been chosen as a reference value in (16), because it has the smallest RMSE and is constant over the widest interval of the considered p range from the considered approximations.

3. Calculation

The equations from the article were validated with the GGD generator [14] with fixed variance to unity and varying shape parameter in the range $p \in \langle 0.3, 3 \rangle$. The values were selected to cover the range of the most typical values in the signal processing applications. RMSE was applied for the comparison of the estimators output. RMSE was calculated from the equation

$$\text{RMSE} = \frac{1}{M} \sum_{i=1}^{M} \frac{(\widehat{p} - p)^2}{p^2}, \quad (17)$$

where $\widehat{p}$ is a value estimated by the model and p is a real value of a shape parameter. M denotes the number of repetitions and was set to $M = 10^4$ for all experiments.

A small sample size may lead to difficulties with the root finding of the ML method (Eq. (7)), therefore, the stop condition was set to $tolX = 1e-4$ and $tolY = 1e-5$, where $tolX$ and $tolY$ are the absolute errors.

The RMSE increase with decreasing sample size for the ML method is depicted in Fig. 2. The curves are plotted for two selected fixed values $p = 1$ and $p = 2$ in the GGD generator. Before the estimation with ML, the sample size was centered twofold: $ML\,med$ – a median value is subtracted from a sample; $ML\,mean$ – a mean value is subtracted from a sample.
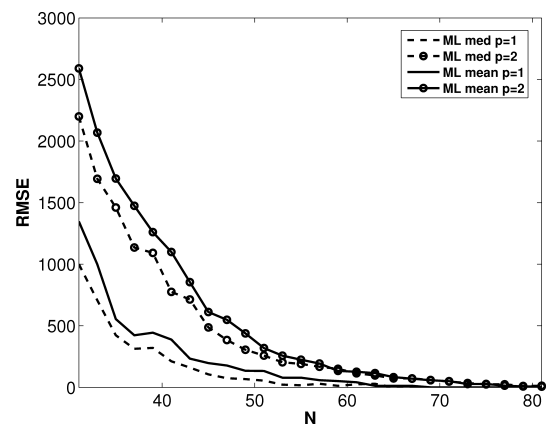

Fig. 2. Comparison of RMSE for the ML method of the estimation of the shape parameter p of GGD with a varying sample size N and for the selected fixed values $p = 1$ and $p = 2$ in the GGD generator. $ML\,med$ – a median value is subtracted from a sample before estimation. $ML\,mean$ – a mean value is subtracted from a sample before estimation

It can be noticed that with a small sample size the ML method resulted in the very high value of error in terms of RMSE (Fig. 2). In the first step, the observation set is centered. It can be done simply by subtracting either the mean value of the set or the median value of the set. It turns out to have influence on the final estimation error. Figure 2 shows that the smaller RMSE is assured by subtracting the median value. The similar behavior for the approximated method (Approx, Eq. (5)) is observed, i.e., the subtraction of a mean value resulted in the higher value of RMSE. In the following, when the results for the Approx and ML methods will be demonstrated, they will be based on the centering using a median.

First, the location parameter μ has to be determined after collecting a sample of GGD random variable. The estimation of the μ parameter can be conducted twofold by: the mean or median. Then it is made centering by subtracting the estimation of the μ parameter. Figure 3 depicts three curves with a median centering for the location parameters in the GGD

generator: $\mu = -1$, $\mu = 0$ and $\mu = 1$ for $\widehat{p_0}$ (Eq. (10)). It can be noticed that these curves overlap.
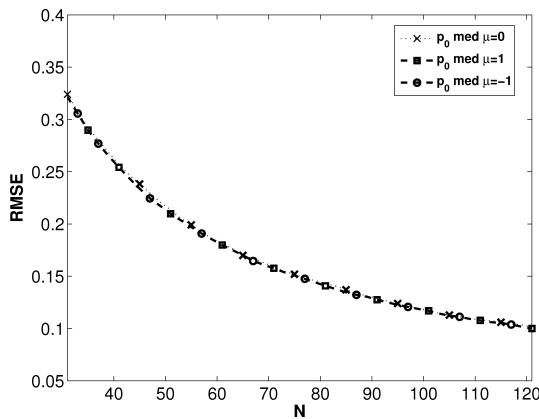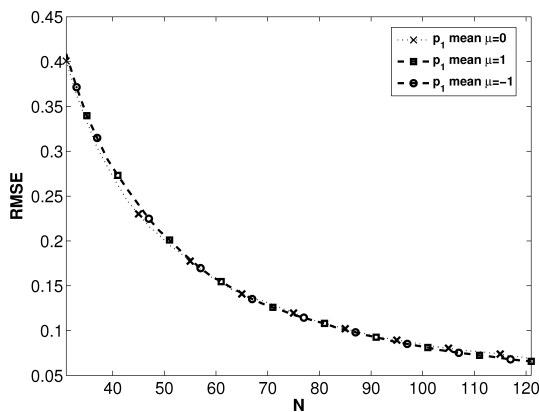

Fig. 3. Comparison of RMSE for the $\widehat{p_0}$ (Eq. (10)) component of the estimation of the shape parameter p of GGD with a varying sample size N and for the selected fixed value $p = 2$ for three location parameters $\mu = -1$, $\mu = 0$ and $\mu = 1$ in the GGD generator and with a median centering

The similar curves with a mean centering for $\widehat{p_1}$ (Eq. (11)) for the location parameters in the GGD generator: $\mu = -1$, $\mu = 0$ and $\mu = 1$ were plotted in Fig. 4. In this case the curves also overlap.

Fig. 4. Comparison of RMSE for the $\widehat{p_1}$ (Eq. (11)) component of the estimation of the shape parameter p of GGD with a varying sample size N and for the selected fixed value $p = 2$ for three location parameters $\mu = -1$, $\mu = 0$ and $\mu = 1$ in the GGD generator and with a mean centering

Figure 5 shows the influence of the median and mean subtraction for two selected components $\widehat{p_0}$ (Eq. (10)) and $\widehat{p_1}$ (Eq. (11)) used in the final equation (Eq. (16)). The median subtraction resulted in the smaller value of RMSE for both $\widehat{p_0}$ (Eq. (10)) and $\widehat{p_1}$ (Eq. (11)) comparing to the mean subtraction.

RMSE for the final equation ($\widehat{p_S}$, Eq. (16)) is depicted in Fig. 6. The curve can be compared to all components of the equation (Eq. (10)–(15)) for the small sample size $N = 31$. A median value is subtracted from a sample before estimation. The method is designed to keep a constant RMSE (at least not increasing) over the considered range of p.
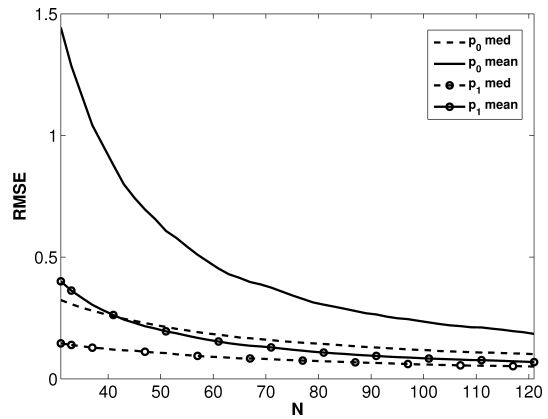

Fig. 5. Comparison of RMSE for the $\widehat{p_0}$ (Eq. (10)) and $\widehat{p_1}$ (Eq. (11)) components of the estimation of the shape parameter p of GGD with a varying sample size N and for the selected fixed value $p = 2$ in the GGD generator. med and $mean$ – a median and mean values are subtracted from a sample before estimation respectively
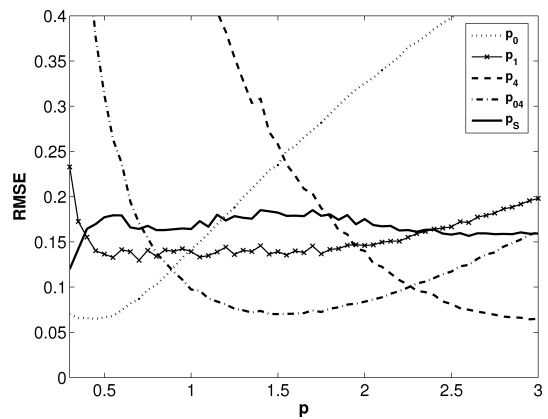

Fig. 6. Comparison of RMSE for both all components (Eq. (10)–(15)) and the final equation ($\widehat{p_S}$, Eq. (16)) of the estimation of the shape parameter p of GGD with a varying shape value p and a selected fixed sample size $N = 31$

A figure for the comparison of RMSE for the $\widehat{p_S}$ (Eq. (16)), ML, Approx methods of the estimation of the shape parameter p of GGD with a varying shape value p and a selected fixed sample size $N = 31$ is not presented in the article due to an excessive error of ML. The smallest N that would be representative to compare the $\widehat{p_S}$ (Eq. (16)), ML, Approx methods was selected $N = 71$. In Fig. 7, it is observed that the Approx method plot is not completed. Upon closer examination the curve discontinuities can be noticed. Such a case denotes when the Approx estimator [6] output has at least one complex value. Thus, RMSE was inapplicable and incomparable. For the ML case, it can be noticed that with increasing values of p in the GGD generator, RMSE increase rapidly with ringing. A median value is subtracted from a sample before estimation.

The global convergence method (GCM) [8] requires to find the root of $Z_n(p) = 0$, which for a small sample size may not have a real root.
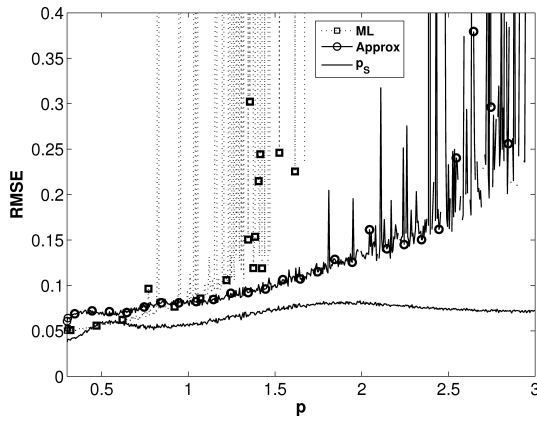
Fig. 7. Comparison of RMSE for $\widehat{p}_S$ (Eq. (16)), ML, Approx methods of the estimation of the shape parameter p of GGD with a varying shape value p and a selected fixed sample size $N = 71$

The similar plot for $N = 121$ is depicted in Fig. 8, whereas expected the RMSE for ML has been reduced. In both cases the introduced estimator (Eq. (16)) behaves stable and the RMSE is the smallest or comparable.
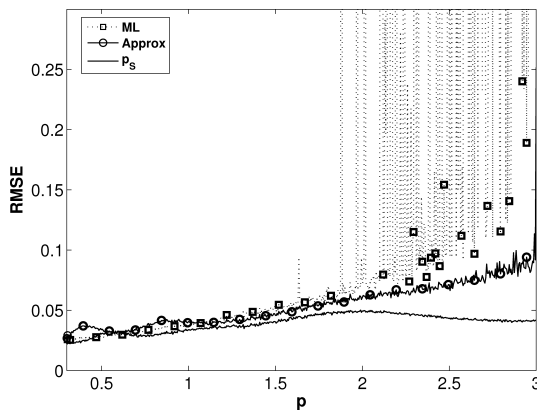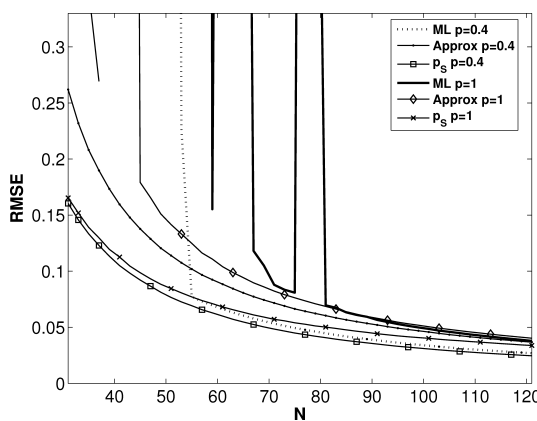

Fig. 8. Comparison of RMSE for $\widehat{p}_S$ (Eq. (16)), ML, Approx methods of the estimation of the shape parameter p of GGD with a varying shape value p and a selected fixed sample size $N = 121$

Fig. 9. Comparison of RMSE for $\widehat{p}_S$ (Eq. (16)), ML, Approx methods of the estimation of the shape parameter p of GGD with a varying sample size N and for the selected fixed values $p = 0.4$ and $p = 1$ in the GGD generator

From Figs. 9 and 10 it can be read that $\widehat{p}_S$ is stable with the small values of N whereas RMSE rapidly grows for ML or get complex for Approx. For these both simulations, the repetition count in Eq. (17) was increased to $M = 10^5$. A median value is subtracted from a sample before estimation.
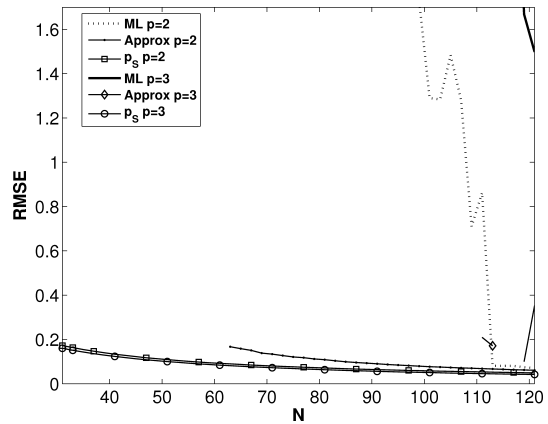

Fig. 10. Comparison of RMSE for $\widehat{p}_S$ (Eq. (16)), ML, Approx methods of the estimation of the shape parameter p of GGD with a varying sample size N and for the selected fixed values $p = 2$ and $p = 3$ in the GGD generator

In Fig. 11, RMSE for $\widehat{p}_S$ when a mean ($\widehat{p}_{S\ mean}$) and median ($\widehat{p}_{S\ med}$) values are subtracted from a sample before estimation is plotted. It can be noted that with the higher values p of the GGD generator subtracting a mean resulted in a smaller value of RMSE. The mean value of these two values $\widehat{p}_{S\ med\ mean} = 0.5 \cdot (\widehat{p}_{S\ mean} + \widehat{p}_{S\ med})$ can give an estimation that will produce the lowest RMSE in short interval around $p = 2$. These curves suggest the combination of them, for instance, $\widehat{p}_{S\ join} = [if\ (\widehat{p}_{S\ med} < 2)$ $then\ (\widehat{p}_{S\ med})\ else\ (\widehat{p}_{S\ med\ mean})]$, but the combined curve $\widehat{p}_{S\ join}$ did not result in better RMSE performance, because of the decision point $\widehat{p}_{S\ med}$ being biased with an error.
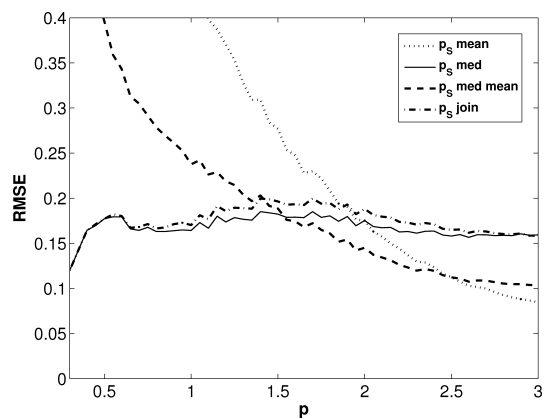

Fig. 11. Comparison of RMSE for the $\widehat{p}_S$ (Eq. (16)) method of the estimation of the shape parameter p of GGD with a varying shape value p and a selected fixed sample size $N = 31$. $\widehat{p}_{S\ med}$ – a median value is subtracted from a sample before estimation. $\widehat{p}_{S\ mean}$ – a mean value is subtracted from a sample before estimation. $\widehat{p}_{S\ med\ mean}$ – a mean p value from estimation $\widehat{p}_{S\ med}$ and $\widehat{p}_{S\ mean}$. $\widehat{p}_{S\ join}$ – a combination of $\widehat{p}_{S\ med}$ and $\widehat{p}_{S\ med\ mean}$

As a limit case it has been considered $N = 1000$ and $N = 2000$ and the results are depicted in Figs. 12 and 13. In this simulation and the following ones, a median value is subtracted from a sample before estimation. RMSE of the ML and Approx methods is stable in the range $p \in \langle 0.3, 3 \rangle$ whereas $\widehat{p}_S$ fluctuates.
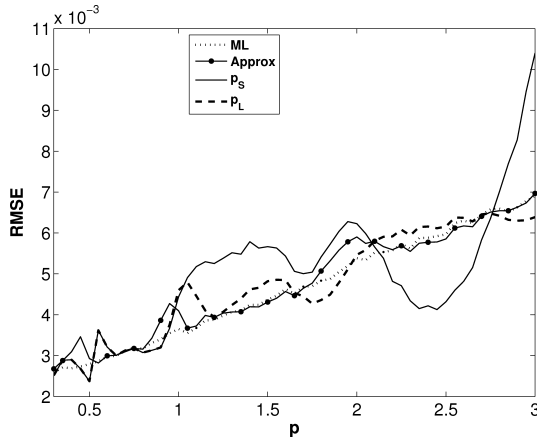

Fig. 12. Comparison of RMSE for the $\widehat{p}_S$ (Eq. (16)), $\widehat{p}_L$ (Eq. (18)), ML, Approx methods of the estimation of the shape parameter p of GGD with a varying shape value p and a selected fixed sample size $N = 1000$

Fig. 13. Comparison of RMSE for the $\widehat{p}_S$ (Eq. (16)), $\widehat{p}_L$ (Eq. (18)), ML, Approx methods of the estimation of the shape parameter p of GGD with a varying shape value p and a selected fixed sample size $N = 2000$
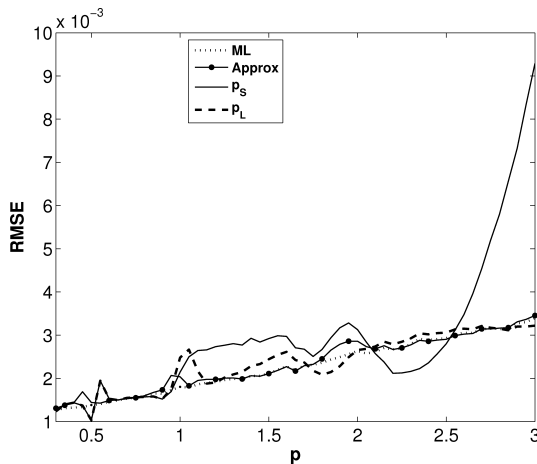
The final estimation $\widehat{p}_L$ with a correction for the larger values of N and p can be found from the following relation:

$$\widehat{p}_L = \begin{cases} \widehat{p}_3, & \text{for } \widehat{p}_1 \geq 1.86 \\ \widehat{p}_2, & \text{for } 1.04 \leq \widehat{p}_1 < 1.86 \\ \widehat{p}_1, & \text{for } 0.57 \leq \widehat{p}_1 < 1.04 \\ \widehat{p}_0, & \text{for } \widehat{p}_1 < 0.57 \end{cases}, \quad (18)$$

where $\widehat{p}_0$, $\widehat{p}_1$, $\widehat{p}_2$ and $\widehat{p}_3$ are defined by Eqs. (10)–(12) and (13) respectively.

For the larger values N, the fluctuation of $\widehat{p}_S$ in the range $p \in \langle 2, 3 \rangle$ can be corrected with the application of $\widehat{p}_L$ (Fig. 13).
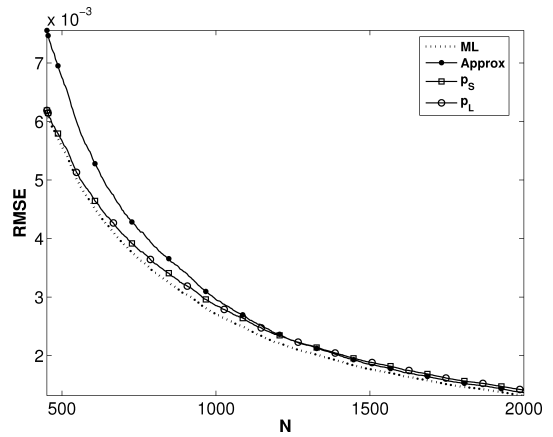

Fig. 14. Comparison of RMSE for the $\widehat{p}_S$ (Eq. (16)), $\widehat{p}_L$ (Eq. (18)), ML, Approx methods of the estimation of the shape parameter p of GGD with a varying sample size N and for the selected fixed values $p = 0.4$ in the GGD generator

Fig. 15. Comparison of RMSE for the $\widehat{p}_S$ (Eq. (16)), $\widehat{p}_L$ (Eq. (18)), ML, Approx methods of the estimation of the shape parameter p of GGD with a varying sample size N and for the selected fixed values $p = 1$ in the GGD generator
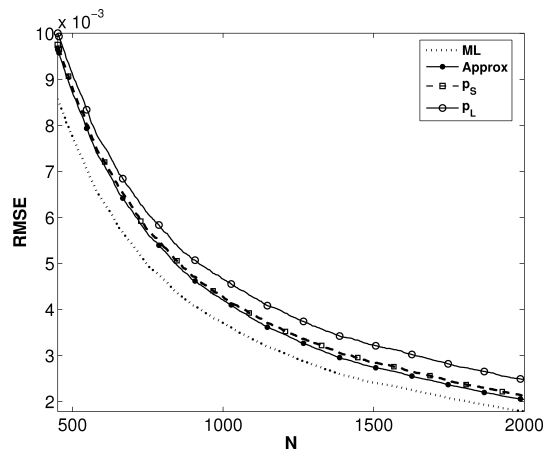

Fig. 16. Comparison of RMSE for the $\widehat{p}_S$ (Eq. (16)), $\widehat{p}_L$ (Eq. (18)), ML, Approx methods of the estimation of the shape parameter p of GGD with a varying sample size N and for the selected fixed values $p = 2$ in the GGD generator
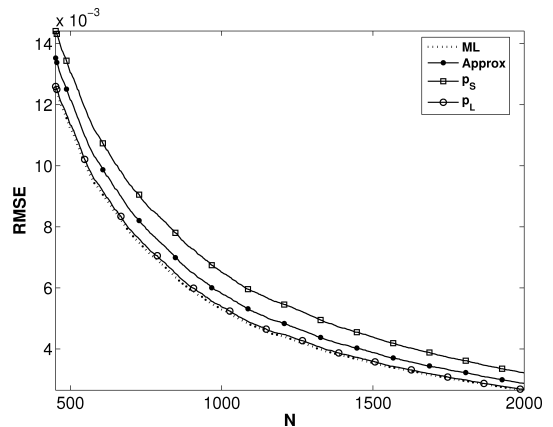
For $N \in (450, 2000)$ and $p = 0.4$, the $\widehat{p}_S$ method gives the comparable results to $\widehat{p}_L$ (Fig. 14).

Other plots $\widehat{p}_S$ and $\widehat{p}_L$ for $N \in (450, 2000)$ and $p = 1$, $p = 2$, $p = 3$ are depicted in Figs. 15, 16 and 17. It is advised to use $\widehat{p}_L$ instead of $\widehat{p}_S$ for the larger values of N and p.
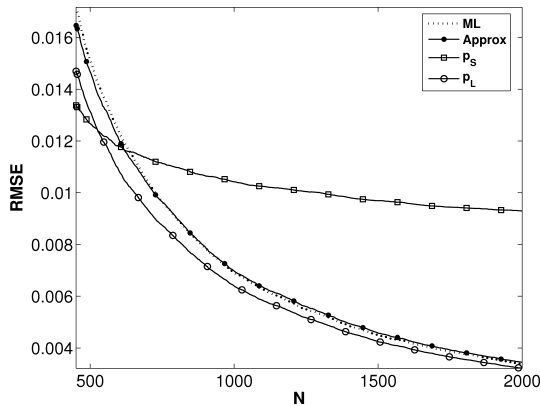

Fig. 17. Comparison of RMSE for the $\widehat{p}_S$ (Eq. (16)), $\widehat{p}_L$ (Eq. (18)), ML, Approx methods of the estimation of the shape parameter p of GGD with a varying sample size N and for the selected fixed values $p = 3$ in the GGD generator

4. Conclusions

The article focuses on the estimation of the shape parameter of GGD when a small size is only available. Most estimation methods for the shape parameter of GGD assume that there is available a set of an unlimited size. In real situations only a set of observations limited in size is usually available. Therefore, the lower the sample size, the higher variance of the estimated value. This also leads to a situation when the already known estimation methods do not have a real root. The method introduced in the article allows to estimate the shape parameter of GGD in the range $p \in \langle 0.3, 3 \rangle$ for a small sample size. Moreover, the method does not require any root finding, any long look-up table or multi step approach, thus, it is simple, fast and relatively efficient. The presented method keeps relatively small RMSE in the range $p \in \langle 0.3, 3 \rangle$ for a small sample size as it was confirmed by simulations whereas other methods had an excessive error in the part of the range, for instance $N = 71$, the ML method for $p > 0.75$, the approximated method for $p > 1.6$. The simulations also exhibited slowly increasing RMSE with the decreasing sample size to $N = 31$ for a new method, where other methods had a jump in RMSE for some threshold sample size. It was observed for the simulations for the shape parameter $p = 0.4$, $p = 1$, $p = 2$ and $p = 3$.

REFERENCES

[1] Y. Du, "Ein sphärisch invariantes Verbunddichtemodell für Bildsignale", *Archiv für Elektronik und Übertragungstechnik*, AEÜ-45 (3), 148–159 (1991).

[2] S.G. Mallat, "A theory of multiresolution signal decomposition: the wavelet representation", *Trans. Pattern Anal. Mach. Intell., IEEE* 11 (7), 674–693 (1989).

[3] B. Aiazzi, L. Alparone, and S. Baronti, "Estimation based on entropy matching for generalized Gaussian PDF modeling", *Signal Process. Lett., IEEE* 6 (6), 138–140 (1999).

[4] S. Meignen and H. Meignen, "On the modeling of small sample distributions with generalized Gaussian density in a maximum likelihood framework", *Image Processing, IEEE Trans.* 15 (6), 1647–1652 (2006).

[5] R. Krupiński and J. Purczyński, "Modeling the distribution of dct coefficients for jpeg reconstruction", *Image Commun.* 22 (5), 439–447, DOI: 10.1016/j.image.2007.03.003 (2007).

[6] R. Krupiński and J. Purczyński, "Approximated fast estimator for the shape parameter of generalized Gaussian distribution", *Signal Process.* 86 (2), 205–211, DOI:10.1016/j.sigpro.2005.05.003 (2006).

[7] M. Novey, T. Adali, and A. Roy, "A complex generalized Gaussian distribution – characterization, generation, and estimation", *Signal Processing, IEEE Trans.* 58 (3), 1427–1433, March (2010).

[8] S. Yu, A. Zhang, and H. Li, "A review of estimating the shape parameter of generalized Gaussian distribution", *J. Comput. Information Systems* 8 (21), 9055–9064 (2012), [Online] available: http://www.jofcis.com/downloadpaper.aspx?id=2756&name=2012_8_21_9055_9064.pdf

[9] T. Marciniak, R. Weychan, A. Stankiewicz, and A. Dąbrowski, "Biometric speech signal processing in a system with digital signal processor", *Bull. Pol. Ac.: Tech.* 62 (2), 589–594, DOI: 10.2478/bpasts-2014-0064 (2014).

[10] M. Mazur, J. Domaradzki, and D. Wojcieszak, "Optical and electrical properties of (Ti-V)O$_x$ thin film as n-type Transparent Oxide Semiconductor", *Bull. Pol. Ac.: Tech.* 62 (3), 583–588, DOI: 10.2478/bpasts-2014-0063 (2014).

[11] G. Box and G.C. Tiao, *Bayesian Inference in Statistical Analysis*, Addison Wesley, New York, 1973.

[12] F.W.J. Olver, *Asymptotics and Special Functions*, Academic Press, New York, 1974.

[13] M.K. Varanasi and B. Aazhang, "Parametric generalized Gaussian density estimation", *J. Acoust. Soc. Amer.* 86 (4), 1404–1415 (1989).

[14] K. Kokkinakis and A.K. Nandi, "Exponent parameter estimation for generalized Gaussian probability density functions with application to speech modeling", *Signal Process.* 85 (9), 1852–1858, DOI:10.1016/j.sigpro.2005.02.017 (2005).